

SEGMENTATION OF PROSTATE CONTOURS FROM ULTRASOUND IMAGES

*P. Abolmaesumi*¹, *M.R. Sirouspour*²

¹School of Computing, Queen's University
Kingston, Ontario, Canada K7L 5M3
purang@cs.queensu.ca

²Department of Electrical and Computer Engineering, McMaster University
Hamilton, Ontario, Canada L8S 4K1
sirouspour@ece.mcmaster.ca

ABSTRACT

This paper presents a novel segmentation technique to extract prostate contours from Transrectal Ultrasound (TRUS) images. A Sticks Filter is first used to reduce the speckle and enhance the image contrast. The problem is then discretized by projecting equispaced radii from an arbitrary seed point inside the prostate cavity towards its boundary. The distance of the prostate boundary from the seed point is modeled by the trajectory of a moving object. The motion of this moving object is assumed to be governed by a finite set of dynamical models subject to uncertainty. Candidate edge points obtained along each radius include the measurement of the object position and some false returns. This modeling approach enables us to employ the interacting multiple model (IMM) estimator along with a probabilistic data association filter (PDAF) for prostate contour extraction. Since the method does not employ any numerical optimization, convergence is very fast. The robustness and accuracy of the method is demonstrated by segmenting contours from a series of prostate ultrasound images.

1. INTRODUCTION

Prostate cancer is the most commonly diagnosed cancer in North America and is the second-leading cause of cancer deaths in elderly men with approximately 33,000 deaths per year [1, 2]. One of the most common imaging modalities that is used to visualize prostate for the purpose of diagnosis and biopsy is TRUS. Although currently, boundary of prostate images are mainly manually outlined on TRUS images by experienced radiologists, however due to poor contrast of these images, missing boundary segmentations, shadows and echo dropouts, the segmentation results are very subjective and vary between different radiologists. Therefore, a segmentation method that could accurately demonstrate the contours of prostate would be of significant importance for many clinical applications [3].

Several prostate segmentation algorithms for ultrasound images have already been proposed in the literature. The method proposed in [3] uses an anisotropic diffusion filter and patient-specific anatomical information to help an expert radiologist to manually segment the images. An algorithm based on quadratic wavelet spline and an active contour model that evolves across

edge maps at different resolutions of wavelet transform to converge to the prostate contour is proposed in [4]. Another approach uses model-based initialization and a discrete dynamic contour [5]. The algorithm requires the user select points on the prostate contour with which an estimate of the prostate shape is interpolated using cubic functions. The algorithm was further extended to segment 3D prostate volumes [6]. A 3D deformable surface is also used in [7] and is demonstrated to be successful in segmenting 3D ultrasound prostate images. Other proposed approaches use Gabor filter texture segmentation [2] and morphological operators [8].

A statistical shape model is reported for automatic prostate segmentation [1]. The algorithm uses a Gabor filter bank in multiple scales and orientations to characterize prostate boundary in TRUS. The proposed method then uses a deformable model that converges to prostate boundary in a coarse to fine approach.

Most of the developed techniques use deformable model concepts in segmenting prostate images. Except [1], which employs an automatic initialization technique, all the other methods use human intervention to get a close guess to the actual boundary for the initialization of the deformable model. In addition, since there is an optimization stage involved, these techniques are usually slow and susceptible to local minimums, very commonly caused by speckle and shadowing effects in ultrasound images. Furthermore, most of the techniques in the literature compromise the processing time for image segmentation in order to achieve a better accuracy in the segmentation results.

We propose a new algorithm for ultrasound image segmentation for which no numerical optimization technique is employed. The method uses the concept of combining multiple trajectory models in order to track a single target in a randomly distributed cluttered environment [9, 10]. In the previous original work by the authors [11], a PDAF technique was used to extract carotid artery contours from a sequence of ultrasound images in real-time. In the current work, we combine the PDAF technique with the IMM estimator in order to increase the accuracy of the extracted contours. This combination has been necessary, since in contrast to the carotid artery that has a well-defined circular shape, prostate boundary can have almost any arbitrary shape and come in different sizes. Because of the low computational cost of the algorithm, it has a great potential to be implemented for real-time applications.

The rest of the paper is organized as follows. Section 2 briefly explains the pre-processing stage for prostate images. Section 3 describes the new IMM/PDAF-based contour extraction tech-

The authors would like to thank IRIS/PRECARN Network of Centres of Excellence and Communications and Information Technology Ontario (CITO) for supporting this project.

nique. Section 4 presents the experimental results. Section 5 discusses the limitations of the algorithm and possible solutions to overcome those. Section 6 concludes the paper with a discussion of the results and future improvements to the algorithm.

2. PREPROCESSING

Due to speckle and artifacts caused by e.g., pubic arch, occlusion of part of prostate due to bowel gas and shadowing effects due to calcification in the prostate [3], prostate contours in ultrasound images are not very clear which makes them very challenging to segment, both for naked human eye as well as any automatic segmentation algorithm. Sticks filter [3, 8] is a very powerful tool to enhance the boundaries in ultrasound images. This filter takes advantage of the fact that speckle in ultrasound images is decorrelated at large distances. The algorithm considers a small square of size $N \times N$ around each pixel in the image. It then finds the line with length N that passes through the central pixel of the square and has the maximum gray-level summation. The algorithm assigns this summation to the central pixel of the square and continues to the next pixel until all the pixels in the image are filtered. Figure 1 shows the implementation results with $N=15$ for a prostate ultrasound image. Note the significant boundary enhancement in the filtered image. We use sticks filter as the pre-processing step for our algorithm.

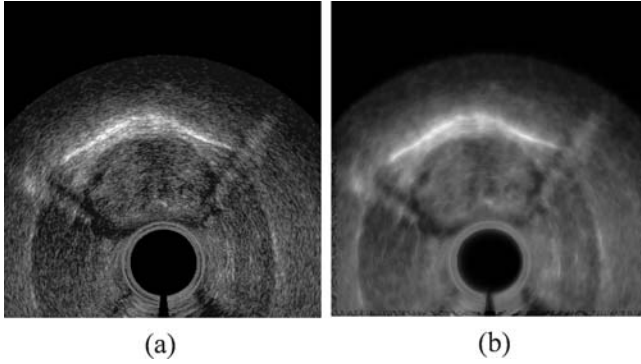


Fig. 1. The result of applying sticks filter on a prostate image; (a) original image (b) filtered image.

3. THE IMM/PDAF ALGORITHM

This section briefly presents a novel image segmentation algorithm to extract prostate boundary from medical images based on the IMM-PDAF state estimator [10]. In this approach, it is assumed that the boundary of the cavity is the trajectory of an object whose motion is governed by a model from a finite set of known models at any given radii. These models can differ in their uncertainty levels and/or their structures. The switching between the models occur according to a set of Markov transition probabilities. The observations are candidate edge points obtained by applying an edge detection algorithm to the pre-filtered image along each radius (see Figure 2). In this research, the following set of approximately constant velocity dynamic models have been employed to

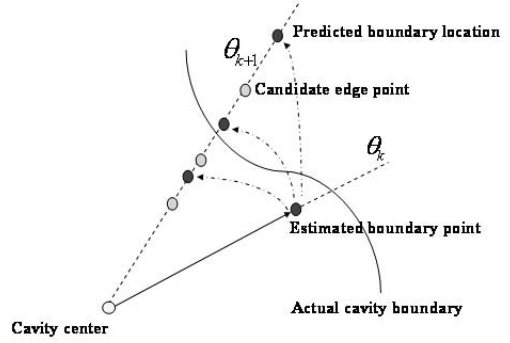


Fig. 2. A schematic diagram of the border extraction method; notations are described in the text.

describe prostate boundary:

$$X_j(k+1) = \begin{bmatrix} 1 & \Delta\theta \\ 0 & 1 \end{bmatrix} X_j(k) + V_j(k) = A_j X_j(k) + V_j(k) \quad (1)$$

$$Z_j(k) = [1 \quad 0] X_j(k) + \omega_j(k) = H_j X_j(k) + \omega_j(k) \quad (2)$$

where $j = 1, \dots, M$, M is the number of trajectory models, $X_j(k) = [d_j(k) \quad d_{\theta j}(k)]^T$ is the system state, $d(k)$ and $d_{\theta}(k)$ are the radius of the prostate boundary from a seed point inside the prostate and its derivative with respect to angle θ , respectively, $\Delta\theta$ is the sampling angle of the prostate boundary from the seed point, $V_j(k)$ is the process noise vector with covariance $Q_j(k) = \begin{bmatrix} \frac{\Delta\theta^4}{4} & \frac{\Delta\theta^3}{2} \\ \frac{\Delta\theta^3}{2} & \Delta\theta^2 \end{bmatrix} \sigma_{v_j}^2$, $Z_j(k)$ is the output of the model, and $\omega_j(k)$ is its error with covariance $R_j(k)$. It is assumed that the acceleration (i.e. the second derivative of the radius with respect to the angle) can be modeled by zero-mean, white, Gaussian noise, and that the model output is a noisy version of the actual position of the prostate boundary given that model j is in effect. Each trajectory model is associated with a Kalman filter and the output of these filters are combined in the recursive IMM/PDAF algorithm [10] to estimate the location of the prostate boundary. Note that although the use of constant velocity models has been found sufficient for prostate contour segmentation however, one can use other dynamic models depending on the application. Note also that unlike standard estimation problems, there are more than one measurement of which only one is assumed to be due to the boundary of the cavity. Therefore, the measurement, $Z(k)$ is defined as (see [9] for details)

$$Z(k) = \sum_{i=1}^{N_c} r_i(k) \beta_i \quad (3)$$

The β_i 's are weighting factors determined by the likelihood of each candidate edge point i on radius k belonging to the boundary. The β_i 's can be computed by assuming that the actual boundary point has a normal distribution with mean $\hat{d}(k|k-1)$, the predicted radius at iteration k . The edge magnitudes are also incorporated in the calculation of the β_i 's such that edges with larger magnitudes would receive a higher weight. Thus, the following formulation is

used to compute the β_i 's:

$$\beta_i(k) = \frac{p_i(k)}{\sum_i p_i(k)} \quad (4)$$

where

$$p_i(k) = \frac{F_{edge}(r_i(k), \theta_k)^2}{\sqrt{2\pi S(k)}} \exp\left(-\frac{(r_i(k) - \hat{d}(k|k-1))^2}{2S(k)}\right) \quad (5)$$

Here, $r_i(k)$ is the distance of the i^{th} candidate edge point along radius k from the seed point with $i = 1, 2, \dots, N_c$, and $F_{edge}(r_i(k), \theta_k)$ is the magnitude of the edge at point $(r_i(k), \theta_k)$ in polar coordinates (see Figure 2). Furthermore, $S(k)$ is the boundary location prediction covariance.

The use of multiple models in the proposed contour extraction algorithm will allow for the automatic adjustment of the filter gain based on the boundary curvature. This is a significant advantage over single-model PDAF which has to compromise between the ability to extract sharp corners, smoothness and sensitivity to noise.

4. EXPERIMENTAL RESULTS

To validate the accuracy and robustness of the proposed algorithm, we tested the method on a series of prostate ultrasound images. The resolution of the images are 512×512 and they are quantized to 256 gray-levels. The current implementation uses two models with $R(k) = 20$ for both of the models and $\sigma_v^2(1) = 10^5$ and $\sigma_v^2(2) = 10^2$ for models one and two, respectively. The number of angularly equispaced radii from a seed point inside each cavity is 512. In the current implementation, the seed points are selected manually by using a mouse pointer. Using MATLABTM, it takes less than 1 s to run the IMM/PDAF algorithm for each image on a 2.4 GHz Pentium 4. For 10 candidate edge points and a maximum radius of 100 pixels for the cavity, the computational complexity of the IMM/PDAF algorithm is in the order of 385 kflops. Figures 3 to 5 show the segmentation results. The algorithm shows an excellent performance in extracting contours of prostate images, even under the existence of shadows and echo dropouts.

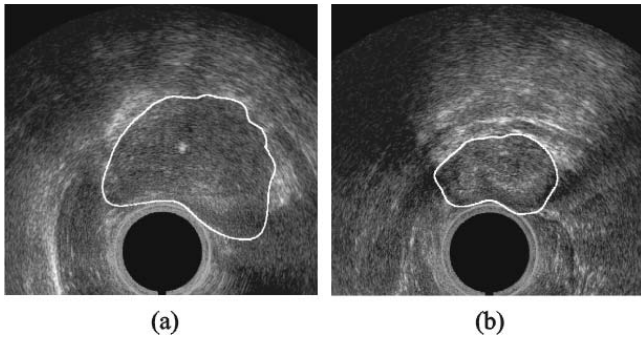


Fig. 3. Segmentation of images 1 and 2.

5. DISCUSSION

In order to evaluate the accuracy of the proposed segmentation algorithm, we asked two expert radiologists to manually segment

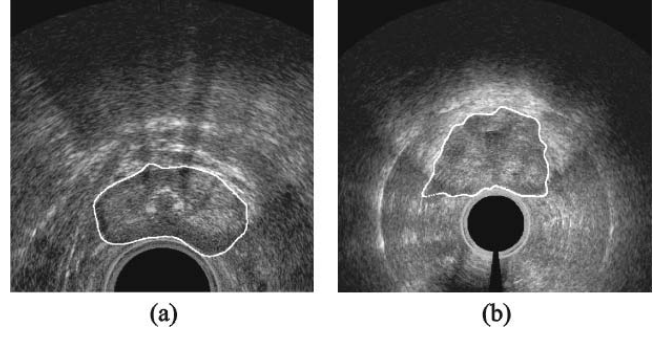


Fig. 4. Segmentation of images 3 and 4.

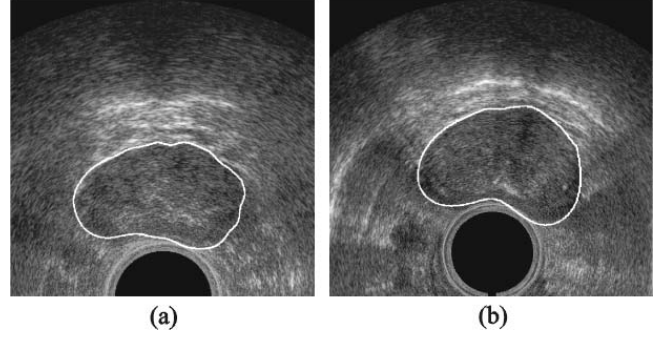


Fig. 5. Segmentation of images 5 and 6.

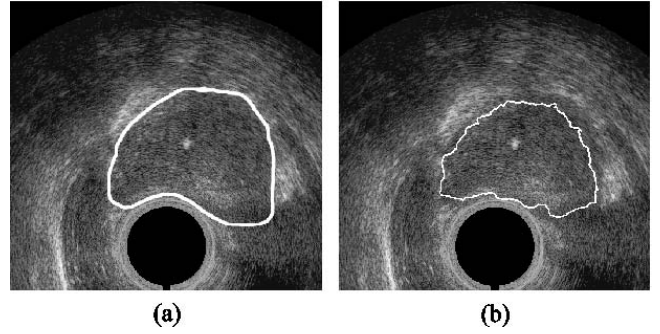


Fig. 6. Comparison of automatic segmentation in Figure 3(a) with: a) Expert's manual segmentation 1; b) Snakes algorithm result.

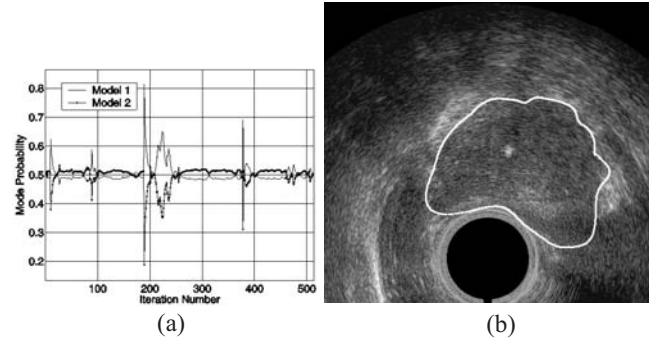


Fig. 7. a) Mode probabilities for the two models used in segmenting Figure 3(a); b) Segmentation of Figure 3(a) using two models with a seed point with coordinates of $y_{seed2} = y_{seed1} - 5$ (pixels).

prostate images. The result for one of the images is demonstrated in Figure 6(a). A quantitative comparison measure that is frequently used in the literature to compare manual and automatic segmentation techniques is the overlapping area of the two techniques. In our 6 sample images, the average overlapping area is 98%. This is comparable to the results previously reported in the literature [1]. Figure 6(b) shows the implementation of the Snakes algorithm on one of the prostate images. As it was mentioned before, the Snakes algorithm is subject to local minimum in the optimization technique as well as close manual initialization of the contour to achieve acceptable results.

In order to provide a better understanding of the way the algorithm works, Figure 7(a) shows the mode probabilities of the two models used in segmenting Figure 3(a) in each iteration. The figure shows that depending on the rate of change in the contour radius with respect to the seed point, the algorithm uses different prediction models at every iteration to filter and segment the boundary points.

The IMM/PDAF algorithm demonstrates excellent segmentation results for different size and shape of prostate in ultrasound images. However, the algorithm has its own limitations in its current form. The main limitation is that there should be a point inside the cavity that can see all the cavity boundary points. Although this condition holds for the majority of prostate images, however it also limits the applications of this method in segmenting more complicated shapes that happen in practice. In addition, one might question the sensitivity of the extracted contour to the location of the seed point. Figure 7(b) demonstrates this by shifting the seed point used in Figure 3(a) by 5 pixels in y direction. It is clear that even with this small shift, there is a slight change in the shape of the contour. This is due to the fact that the candidate edge points are detected along one dimensional radii from the seed point and the orientations of these radii change with respect to the actual edge locations when the seed point is displaced. Further research is currently underway to reduce the sensitivity of the algorithm with respect to the position of the seed point.

6. CONCLUSION

This paper presented a novel image segmentation algorithm that uses an interactive multi-model probabilistic data association filter to successfully segment prostate contours from ultrasound images. The application of the algorithm has been demonstrated for different prostate ultrasound images. While maintaining excellent accuracy in extracting details of cavity contours, the filter also produces smooth segmentation results. Since the algorithm does not use any numerical optimization technique, it can be implemented very efficiently and has little computational cost. The next stage of this research will include the development of a fully-automatic algorithm to select seed points inside the prostate cavity instead of operator interventions. Also, the algorithm will be modified to segment non-convex shape cavities.

7. ACKNOWLEDGMENT

The authors wish to thank Dr. N.W. Sing from Nanyang Technological University, Singapore and Dr. D. Shen from University of Pennsylvania to provide us with the prostate ultrasound images. We also would like to thank Dr. P. Fenton and E. Sauerbrei to help us with the manual segmentation of the images.

8. REFERENCES

- [1] D. Shen, Y. Zhan, and C. Davatzikos, "Segmentation of prostate boundaries from ultrasound images using statistical shape model," *IEEE Trans. Med. Imag.*, vol. 22, no. 4, pp. 539–551, 2003.
- [2] S.S. Mohamed, T.K. Abdel-galil, M.M.A. Salma, A. Fenster, D.B. Downey, and K. Rizkalla, "Prostate cancer diagnosis based on gabor filter texture segmentation of ultrasound image," *IEEE CCECE*, pp. 1485–1488, 2003.
- [3] S.D. Pathak, D.R. Haynor, and Y. Kim, "Edge-guided boundary delineation in prostate ultrasound images," *IEEE Trans. Med. Imag.*, vol. 19, no. 12, pp. 1211–1219, 2000.
- [4] F. Zhao and C.J.S. deSilva, "Contour extraction in prostate ultrasound images using the wavelet transform and snakes," *Proc. Intl. Conf. Eng. Med. Bio.*, vol. 3, pp. 2641–2644, 2001.
- [5] H.M. Ladak, F. Mao, Y. Wang, D.B. Downey, D.A. Steinman, and A. Fenster, "Prostate segmentation from 2d ultrasound images," *Proc. Intl. Conf. Eng. Med. Bio.*, vol. 4, pp. 3188–3191, 2000.
- [6] N. Hu, D.B. Downey, A. Fenster, and H.M. Ladak, "Prostate surface segmentation from 3d ultrasound images," *Proc. IEEE Intl. Symp. Biomed. Imag.*, pp. 613–616, 2002.
- [7] A. Ghanei and H. Soltanian-Zadeh, "A discrete curvature-based deformable surface model with application to segmentation of volumetric images," *IEEE Trans. Inform. Tech. Biomed.*, vol. 6, no. 4, pp. 285–295, 2002.
- [8] J. Awad, T.K. Abdel-Galil, M.M.A. Salama, A. Fenster, K. Rizkalla, and D.B. Downey, "Prostate's boundary detection in transrectal ultrasound images using scanning technique," *IEEE CCECE*, pp. 1199–1202, 2003.
- [9] Y. Bar-Shalom and T.E. Fortmann, *Tracking and Data Association*, Academic Press Inc., 1988.
- [10] T. Kirburajan, Y. Bar-Shalom, W.D. Blair, and G.A. Watson, "IMMPDAF for radar management and tracking benchmark with ECM," *IEEE Trans. Aerospace and Electronic Systems*, vol. 34, no. 4, pp. 1115–1134, 1998.
- [11] P. Abolmaesumi, S.E. Salcudean, W.H. Zhu, M.R. Sirouspour, and S.P. DiMaio, "Image-guided control of a robot for medical ultrasound," *IEEE Trans. Robot. Autom.*, February 2002.